J. Fluid Mech. (1981), *vol.* 109, *pp.* 283–299
Printed in Great Britain

Experimental study of high-Rayleigh-number convection in a horizontal cavity with different end temperatures

By ADRIAN BEJAN, ADNAN A. AL-HOMOUD
Department of Mechanical Engineering, University of Colorado, Boulder, Colorado, USA
AND JORG IMBERGER
Department of Civil Engineering, University of Western Australia, Nedlands, Australia

(Received 7 December 1979 and in revised form 8 December 1980)

The paper summarizes results from an experimental study of buoyancy-induced motion and heat transfer in a horizontal rectangular cavity with the two vertical ends at different temperatures and the long horizontal walls adiabatic. The cavity height/length ratio is $A = 0{\cdot}0625$. The high-Rayleigh-number range reported on in this paper, $2 \times 10^8 < Ra < 2 \times 10^9$, has not been studied before. It is shown that, contrary to lower-Rayleigh-number behaviour known previously, the core flow structure is non-parallel and is dominated by horizontal intrusions flowing along each of the two insulated horizontal walls of the enclosure. The fluid embraced by the two horizontal jets is practically stagnant and thermally stratified. Flow visualization experiments suggest that adjacent to the two horizontal jets two secondary flat cells are formed by the baroclinic pressure field in an analogous way to what is observed in intrusions in a stratified fluid. Nusselt-number–Rayleigh-number results for the overall end-to-end heat transfer in the horizontal direction are reported and compared with previous experimental and theoretical results available for lower Rayleigh numbers. It is shown also that the transition from a parallel core structure to one dominated by intrusion layers is governed by the parameter $Ra^{\frac{1}{4}}A$, with $Ra^{\frac{1}{4}}A < 1$ as necessary condition for a parallel core flow.

1. Introduction

The phenomenon of natural convection in enclosures is receiving considerable attention owing to its many practical applications. For example, in engineering this class of phenomena plays an important role in the performance of thermal insulations for buildings, solar collectors, cooling systems for nuclear reactors and superconducting magnets. In addition to engineering applications, natural convection is an important mechanism in geophysics and astrophysics.

The flow in a rectangular cavity with the two vertical walls maintained at different temperatures has been studied extensively. However, the vast majority of these studies considered rectangular cavities with the height H much greater than length L. The initial work on this specific geometry was inspired by the interest in heat leaks through double-pane windows, and was pioneered theoretically by Batchelor (1954)

and experimentally by Eckert & Carlson (1961). A comprehensive review of the work on free convection in tall enclosures was assembled by Ostrach (1972).

In view of the wealth of information published on tall cavities, it is surprising to see how little has been done to uncover the convection mechanism in horizontal cavities with different end temperatures ($H/L \ll 1$). In a three-paper sequence, Cormack, Leal & Imberger (1974), Cormack, Leal & Seinfeld (1974) and Imberger (1974) have addressed this question. These authors presented an asymptotic solution valid in the limit $H/L \to 0$ and a fixed Rayleigh number $Ra = \alpha \Delta T g H^3/\nu\kappa$ and Prandtl number $Pr = \nu/\kappa$, where α is the thermal coefficient of expansion, ΔT is the temperature differential, g is the acceleration due to gravity, ν is the kinematic viscosity coefficient and κ is the thermal diffusivity. Imberger (1974) presented experimental results for water with $H/L = 0{\cdot}01$, $0{\cdot}02$ in the range $1{\cdot}31 \times 10^6 \leqslant Ra \leqslant 1{\cdot}11 \times 10^8$. Numerical studies have been reported by Cormack *et al.* (1974), Boyack & Kearney (1972), Tseng (1979) and Sernas & Lee (1978), but all are restricted to a Rayleigh number less than 10^8. Kumar & Ostrach (1977) and Loka (1979) reported experiments in the range $10^4 \leqslant Ra \leqslant 1{\cdot}8 \times 10^7$, $0{\cdot}05 \leqslant A \leqslant 0{\cdot}5$, with special emphasis on the effect of Prandtl number which varied from $0{\cdot}72$ to 1400. The reader can find an overview of these two experiments in a paper presented recently by Ostrach, Loka & Kumar (1980).

The experimental and numerical evidence presented in the above studies reveals an orderly transition of flow regimes as the Rayleigh number is increased from zero to 10^8. At very low Rayleigh numbers horizontal heat conduction is the dominant process. From the results of Imberger (1974) it follows that the transfer of heat by conduction is of the order of $BH\kappa\Delta T/L$ and that due to convection is of the order of $\alpha g H^3 \Delta T^2 BH/\nu L$, where B is the cavity width. Hence, diffusion predominates for $Ra < 1$. In this limit the end walls merely act to turn the weak gravitational circulation through 180° to form a slowly moving gyre in the cavity. The flow over the greater part of the cavity is parallel and driven by the linear horizontal temperature gradient established by the horizontal diffusion.

This core solution remains valid for $Ra > 1$, but convection predominates which in turn intensifies the vertical temperature gradient in the cavity (see Imberger 1974). At the ends the convection leads to the formation of a vertical boundary layer of thickness $(Pr^{\frac{1}{2}} H Ra^{-\frac{1}{4}})$, as shown by Braun, Ostrach & Heighway (1961) and Gill (1966). Hence, the vertical boundary layer will become distinct for $Ra > Pr^2$; the flow near the end regions departs increasingly from the parallel-flow solution discussed by Imberger (1974), and the temperature drop across the vertical boundary layer increases to $\frac{1}{2}\Delta T$, correspondingly weakening the gradient driving the parallel flow near the centre of the cavity. The results presented in Imberger (1974), $Pr^2 = 49$, show: little departure from parallel flow for the case $Ra = 1{\cdot}3 \times 10^6$, half the central cavity filled with parallel flow at $Ra = 8 \times 10^6$ and no parallel flow remaining at $Ra = 1{\cdot}1 \times 10^8$.

The transition to the non-parallel flow case may be estimated from a simple scaling argument. In the parallel flow, the heat imparted to the fluid at the vertical boundary is convected into the cavity by the upper horizontal intrusions. This gain in heat is offset by vertical diffusion into the lower (colder) opposing intrusion entering the cavity from the cold end. This balance is possible as long as the diffusion mechanism is capable of transferring the necessary quantity of heat. The flow in the vertical

boundary layer was shown by Gill (1966) to be $O(\kappa Ra^{\frac{1}{4}})$, so that the convective heat transfer across the box is $O(\kappa \Delta T Ra^{\frac{1}{4}})$, while the maximum diffusive heat flux is $O(\kappa \Delta T L/H)$. Thus the parallel flow mechanism should be present for $Ra < A^{-4}$, where $A = H/L$ is the aspect ratio.

It should be noted that parameter $Ra A^4$ appearing in this transition criterion differs from the group $Ra^2 A^3$ suggested by Cormack *et al.* (1974) as the parameter governing the departure from fully developed parallel core structure. Close inspection of Cormack *et al.*'s $A \to 0$ asymptotic theory reveals that $Ra^2 A^3$ governs only the first-order correction to the parallel core structure known to exist in the $A \to 0$ limit. Unlike $Ra^2 A^3$, parameter $Ra A^4$ dictates the transition to a well-defined, fundamentally different, core counterflow, one which is effected via horizontal intrusions (jets) documented in the present experiment.

For $Ra = A^{-4}$ the end jet intrusion structure found by Imberger (1974) should just penetrate to the central part of the cavity and the temperature along the mid depth should become constant. In the experiment of Imberger (1974) this transition was observed at a Rayleigh number between 10^6 and 10^8 with a A^{-4} equal to 10^7.

In summary, our understanding of the physics seems to be borne out by experimental observations, and there are flow transitions at Ra equal to 1, Pr^2 and A^{-4}. The present study is concerned with the flow for $Ra > A^{-4}$.

Once again it is possible to use simple scaling arguments to predict critical flow transitions. As the Rayleigh number is increased beyond A^{-4}, vertical diffusion across the horizontal intrusions will diminish relative to the horizontal advection of heat and the isotherms will tend to become more horizontal. Since the diffusive flux is unimportant in this limit, it is possible to use Koh's (1976) result for the thickness δ of the horizontal viscous intrusion with $\delta = O(L Ra^{-\frac{3}{16}} A^{\frac{3}{4}})$ (see table 2 in Koh 1976, p. 2959). According to Gill (1966), the horizontal advection of heat is $O(\kappa Ra^{\frac{1}{4}} \Delta T)$, while the vertical diffusion is $O(\kappa \Delta T L/\delta)$. The two estimates balance when $Ra = A^{-12}$. Hence, once this value is reached the upper and lower layers will be viscous intrusions with little vertical heat loss and they will most likely exhibit weak counter-jet behaviour as discussed in Imberger, Thompson & Fandry (1976).

Increasing the Rayleigh number still further, beyond A^{-12} and beyond the limits of the present experiments, will lead to little qualitative change. The viscous intrusions will be replaced by inertial intrusions at a $Ra = Pr^{16} A^{-12}$, which will intensify the intrusions, but cause little noticeable change in the flow patterns.

In conclusion, the objective of the present article is to report representative results from an experimental study conducted in a Rayleigh-number range well above A^{-4}. The water experiment described by Imberger (1974) showed the transition to the limit A^{-4} where the temperature along the centre of the cavity just became uniform and the core flow departed from the parallel counter-flow structure predicted theoretically and verified by lower Ra experiments and numerical simulations. This departure from a truly parallel core structure was again encountered experimentally by Kumar & Ostrach (1977).

In the present experiment the Rayleigh number was increased to roughly twenty times the highest value achieved previously by Imberger (1974). The experiment was designed specifically to permit the study of the thermal convection mechanism in the core section of the enclosure, away from the short vertical ends. We demonstrate that above approximately $Ra = 10^9$ the core flow structure becomes strongly non-

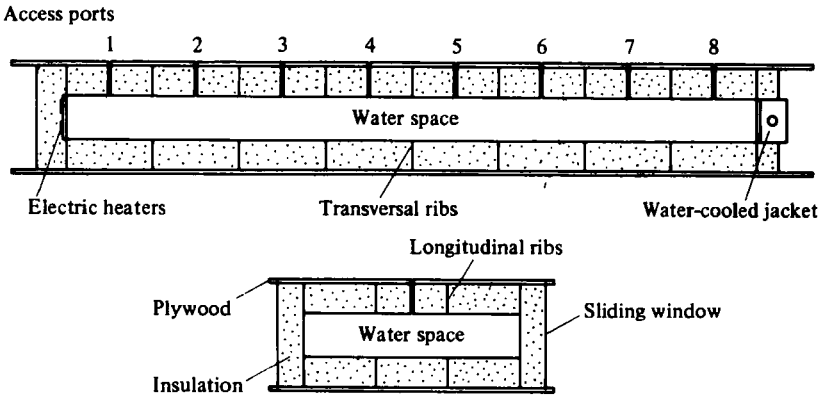

FIGURE 1. Schematic drawing showing longitudinal and transversal cross-sections through the experimental apparatus.

parallel and the isotherms become basically horizontal as predicted: the new feature of the core flow is the presence of two horizontal jets flowing along the upper and lower adiabatic walls, while for most of its depth the cavity is filled with stagnant and thermally stratified fluid. The horizontal jet intrusions set up baroclinic pressure fields adjacent to the primary jet which leads to the formation of two weak elongated cells embraced by the much stronger primary-jet counter-flow present in the core region.

2. Experimental apparatus

A schematic diagram of the apparatus used in this experiment is presented in figure 1. The innermost compartment of the apparatus is a water-filled parallelepipedic cavity 243·8 cm long, 75·6 cm wide and 15·24 cm tall. The cavity aspect ratio is therefore $H/L = 0{\cdot}0625$. The enclosure material is Plexiglas sheet with a thickness of 0·64 cm. The water space lies between two parallel spaces filled with fibreglass insulation. Each of these spaces is 10·2 cm high and is divided by vertical Plexiglas partitions into 30 × 25 cm subspaces. The chief function of these partitions is to provide adequate stiffness to the large horizontal walls (ceiling and floor) of the enclosure. The Plexiglas structure is sandwiched between two sheets of plywood 350·6 × 96·6 cm. Longitudinal grooves were milled near the long edges of the plywood sheets and into these grooves slide two 350 × 35·6 cm Plexiglas windows. For heat-transfer measurements the space created between the lateral windows and the water cavity was filled with fibreglass. During the flow visualization phase of the study the lateral insulation was removed. In this configuration the sliding windows ensured fog-free surfaces for photographing the observed velocity profiles (see §4).

The vertical end-walls of the water space were made out of copper plate with a thickness of 1·27 cm. Both end plates have the rectangular shape of the transversal cross-section through the cavity, 75·6 cm × 15·24 cm. Each plate was brazed to a rectangular stainless steel frame which was later screwed onto the rectangular edge formed by the four Plexiglas walls enclosing the water space. A rubber gasket was placed between the steel frame and the Plexiglas. Owing to the large size and extreme

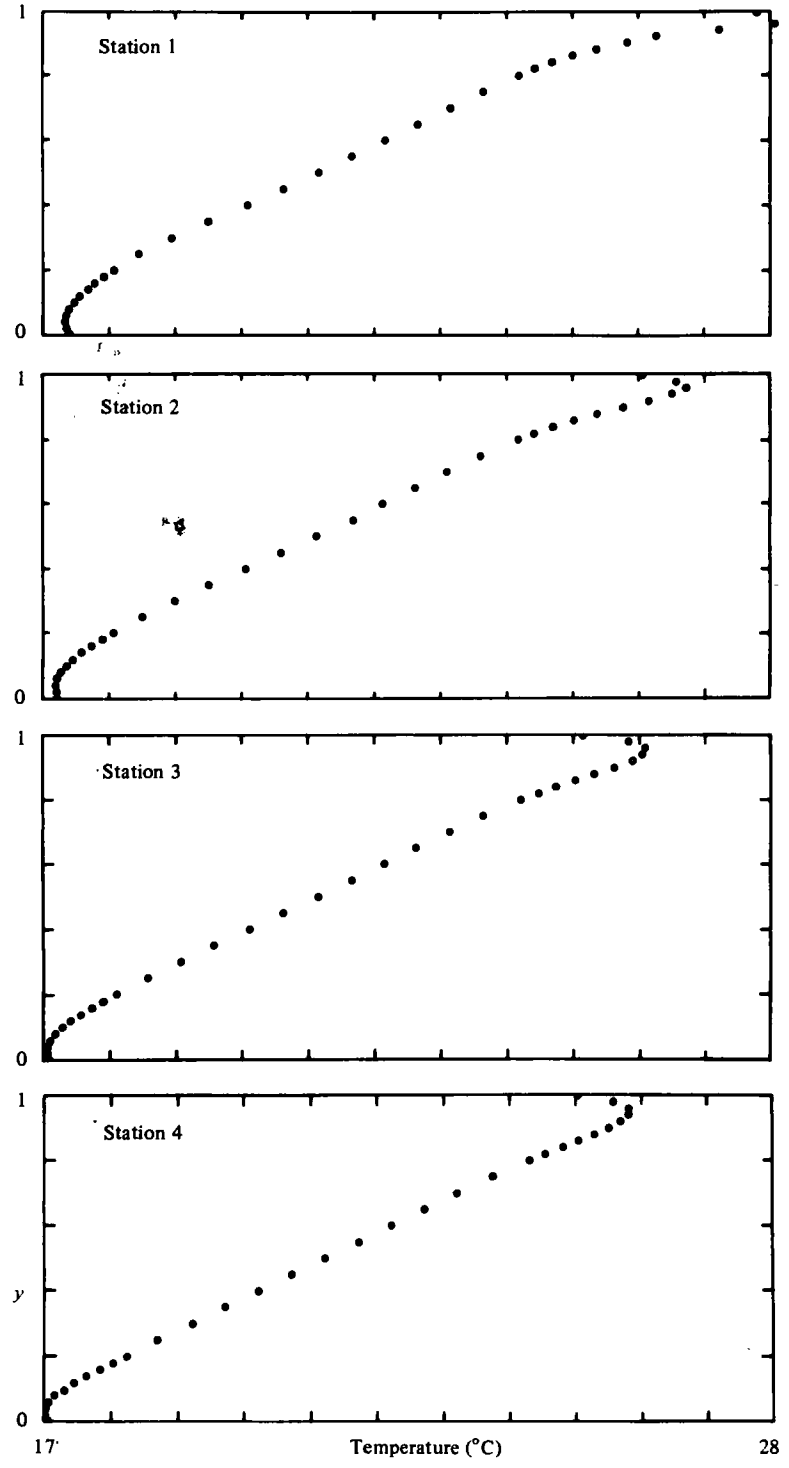

FIGURE 2. Vertical temperature profiles, $Ra = 1{\cdot}22 \times 10^9$, $T_h = 32{\cdot}4$ °C, $T_c = 10{\cdot}5$ °C, for stations 1–8.

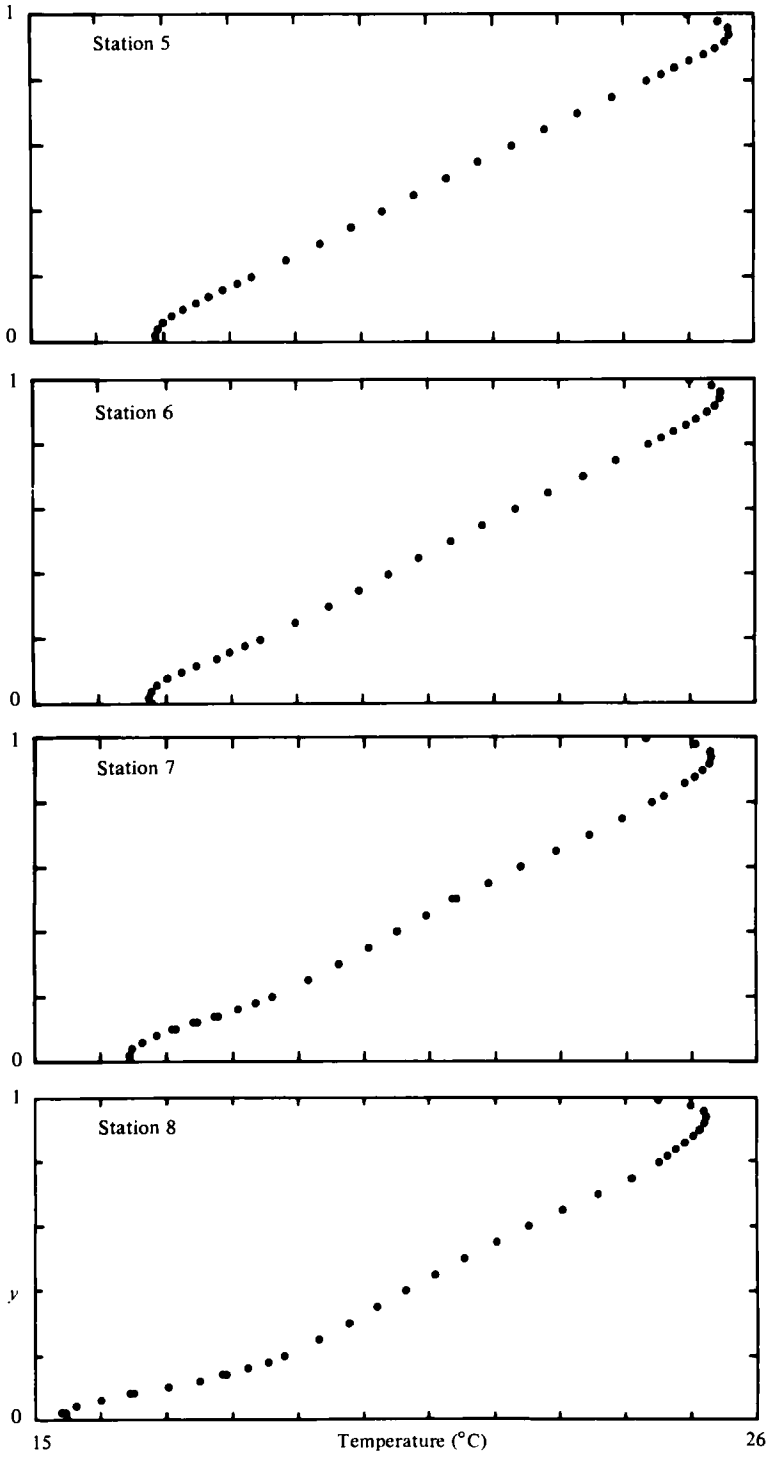

FIGURE 2. For legend see p. 287.

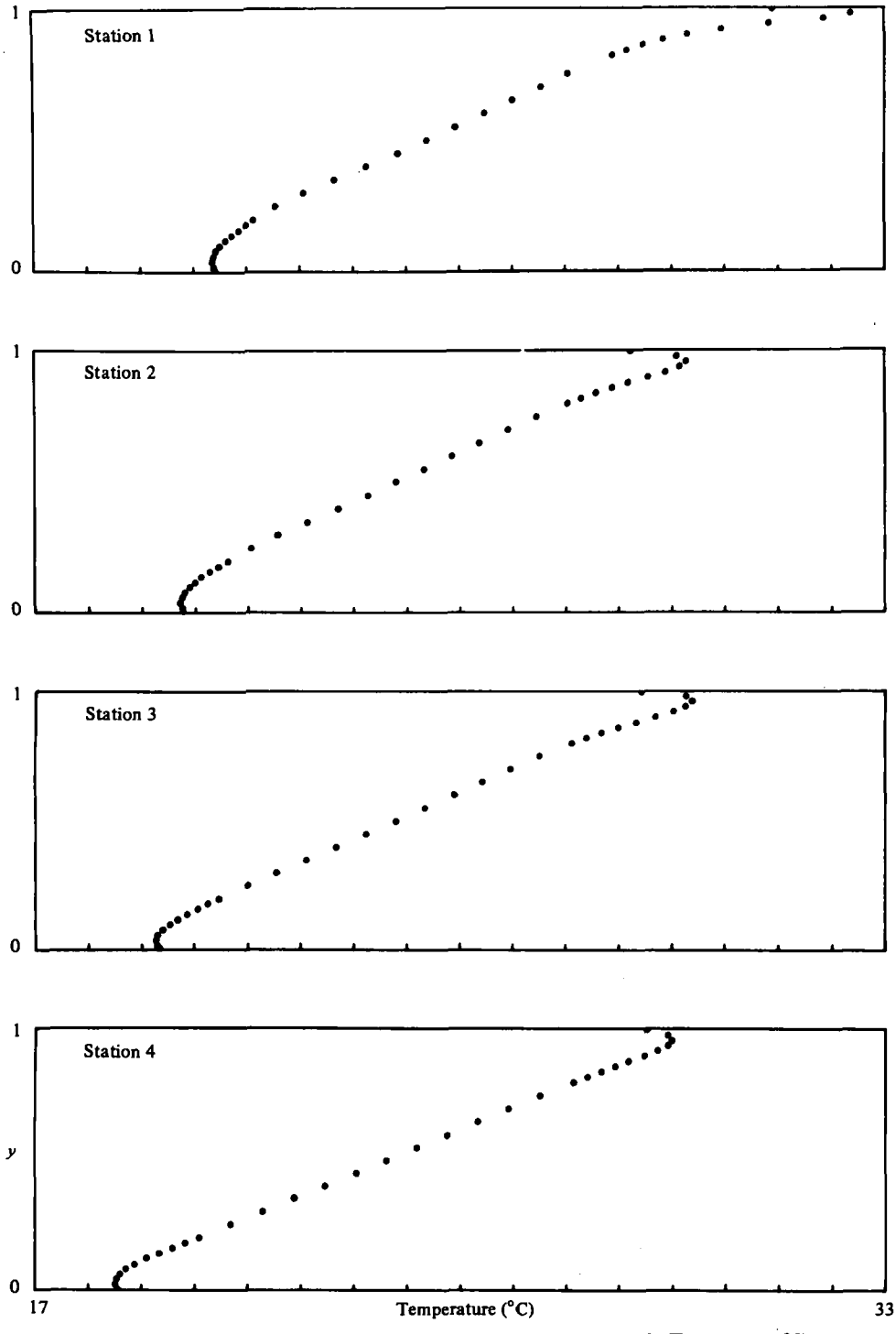

FIGURE 3. Vertical temperature profiles, $Ra = 1{\cdot}59 \times 10^9$, $T_h = 36{\cdot}04$ °C, $T_c = 12{\cdot}04$ °C, for stations 1–8.

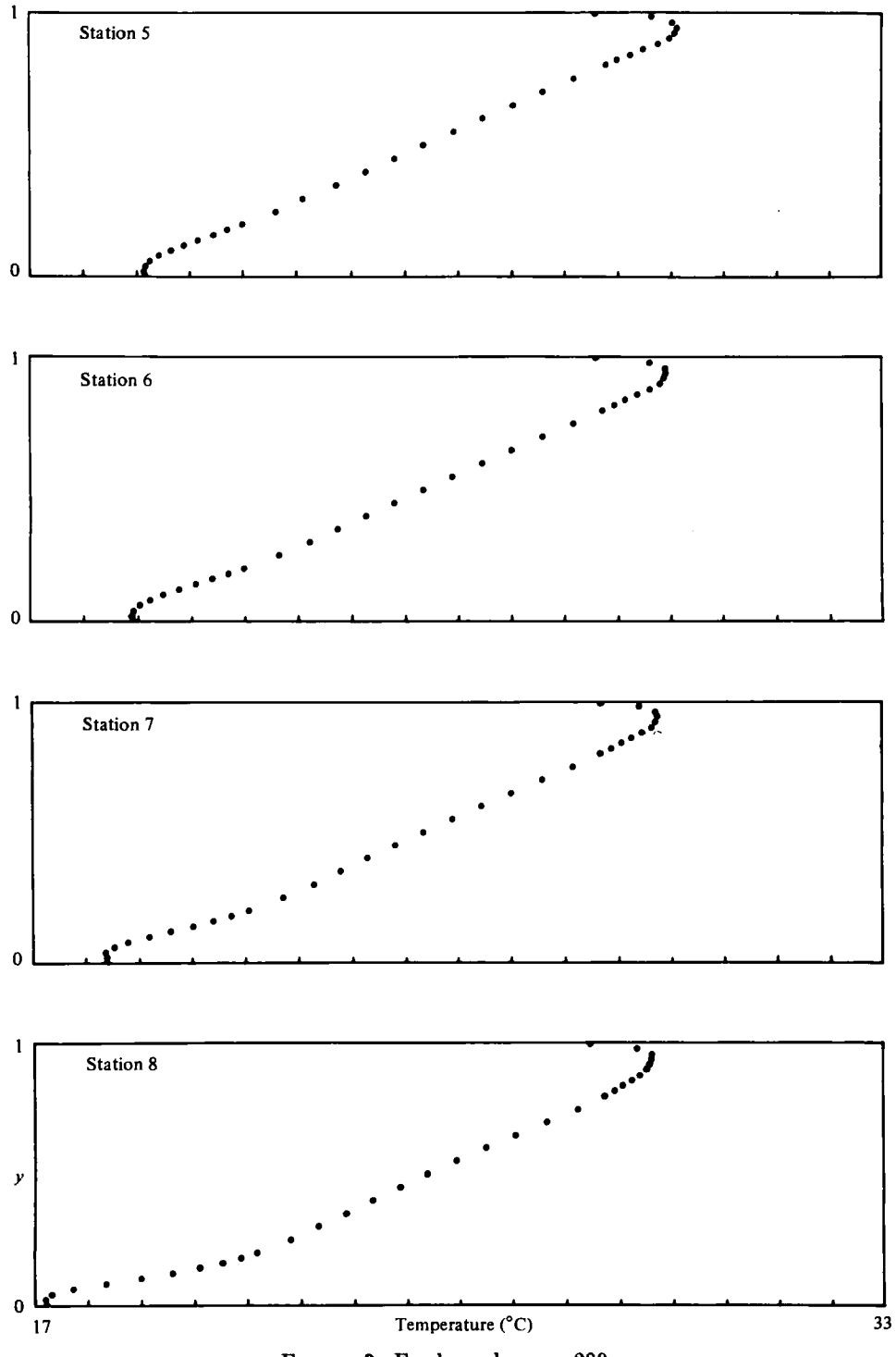

FIGURE 3. For legend see p. 289.

slenderness of the apparatus, minor water leaks were encountered in the early stages of this work.

The thick copper end-plates ensure uniform temperatures for both ends of the cavity. The cold end-plate was fitted with a water-cooled jacket. The water stream is led into the jacket through a horizontal pipe positioned parallel to the copper end-plate. The horizontal pipe has a series of orifices facing the copper plate; through these orifices the cooling stream is divided and sprayed perpendicularly onto the cold end of the cavity. The warm end was heated with a pair of electric strip heaters clamped tight to the copper plate. The reverse side of these heaters was covered with an asbestos sheet and a 10 cm thick fibreglass blanket. The maximum heat input delivered by the electric heaters is 500 W.

To study the temperature and flow pattern in the water cavity, eight access ports (measuring stations) were constructed along the centre-line of the upper wall. The distance between the centres of two adjacent ports is 30·4 cm, while the distance between each extreme port and the end wall is 15·24 cm. Stainless steel tubes 9 cm long and with an inside diameter of 4 mm were mounted vertically into the top Plexiglas wall. In presenting the experimental results which follow we assigned a number to each station, station 1 being the one closest to the heated end (see figure 1). In addition to the eight access ports, the water space has a fill port in the upper wall and a drain: both openings have a diameter of 1·33 cm.

The experiments were performed using distilled water in the long horizontal cavity. For these Rayleigh numbers the characteristic spin-up time is given by $HL/\kappa Ra^{\frac{1}{4}}$ $\sim$ 10 hours. A succession of steady states was achieved by varying the heat input of the warm end over a number of days, while keeping the water-cooled cold end. A conscious effort was made to operate with end temperatures whose arithmetic average came close to the room air temperature. This was necessary in order to minimize the net heat loss through the large horizontal walls of the cavity. As we point out in §5, the maximum heat loss associated with the horizontal walls occurred when the heat input to the warm end was maximum. At that point the heat loss was no more than 9% of the total heat input. The sharp temperature gradient at the top wall (figures 2, 3) is a local heat loss feature due to the fin cooling introduced by each of the eight steel access tubes (numbered 1–8).

Another source of concern was presented by fluctuations encountered in the cold-end temperature and the electric power dissipated in the warm-end resistors. The cold-end temperature fluctuations were due to daily fluctuations of the order of $\pm$ 1·6 °C in the building water supply which was used to feed the water jacket shown in figure 1. These fluctuations were reduced to $\pm$ 0·9 °C by precooling the jacket water stream in a heat exchanger immersed in the ice basket of an ice machine. Since in most circumstances the end-to-end temperature difference was of the order of 15 °C or higher, this variation in the cold-end temperature was considered acceptable. The fluctuations in the heat input to the warm end were caused by changes in the building voltage supply, changes which occurred primarily between weekdays and weekends. These fluctuations were reduced to $\pm$ 1·5 per cent by installing a constant-voltage transformer (Sola) between the building voltage supply and the electric heaters.

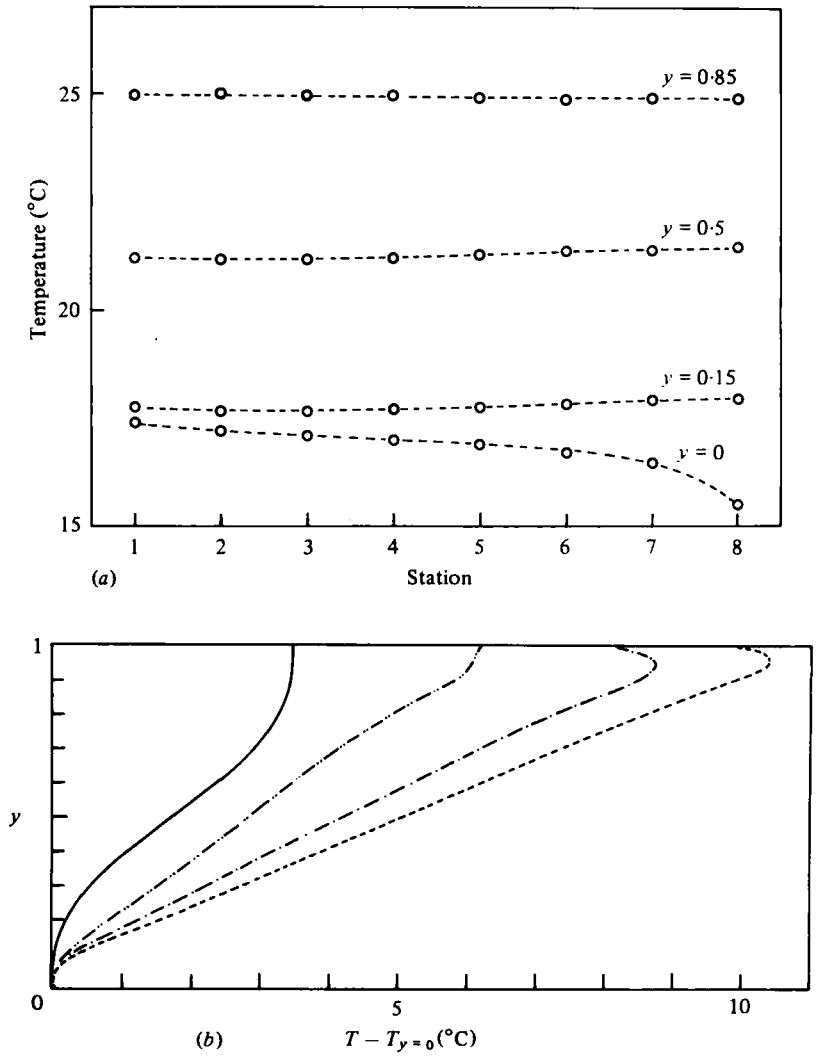

FIGURE 4. (*a*) Temperature *vs.* horizontal position. (*b*) The development of an inner, linearly stratified, region with increasing *Ra*, station 4. – – –, $Ra = 1{\cdot}59 \times 10^9$; – · – · –, $1{\cdot}22 \times 10^9$; – ·· – ·· –, $8{\cdot}41 \times 10^8$; ——, 2×10^4 (enlarged 50 000 times).

3. Temperature measurements

Figures 2 and 3 summarize two sets of measurements for the temperature distribution in the core of the two-dimensional cavity. These measurements were obtained using a variable-depth temperature probe which was lowered through each of the *eight* access ports. The probe consisted of a bead-in-glass precision thermistor mounted at the lower end of a rack-and-pinion mechanism. The thermistor bead diameter was approximately 0·5 mm and its electrical resistance was measured within 0·1 per cent with a digital ohmmeter.

The results of figures 2 and 3 show that except for two thin layers near the top and bottom walls the core fluid is thermally stratified, the vertical temperature gradient

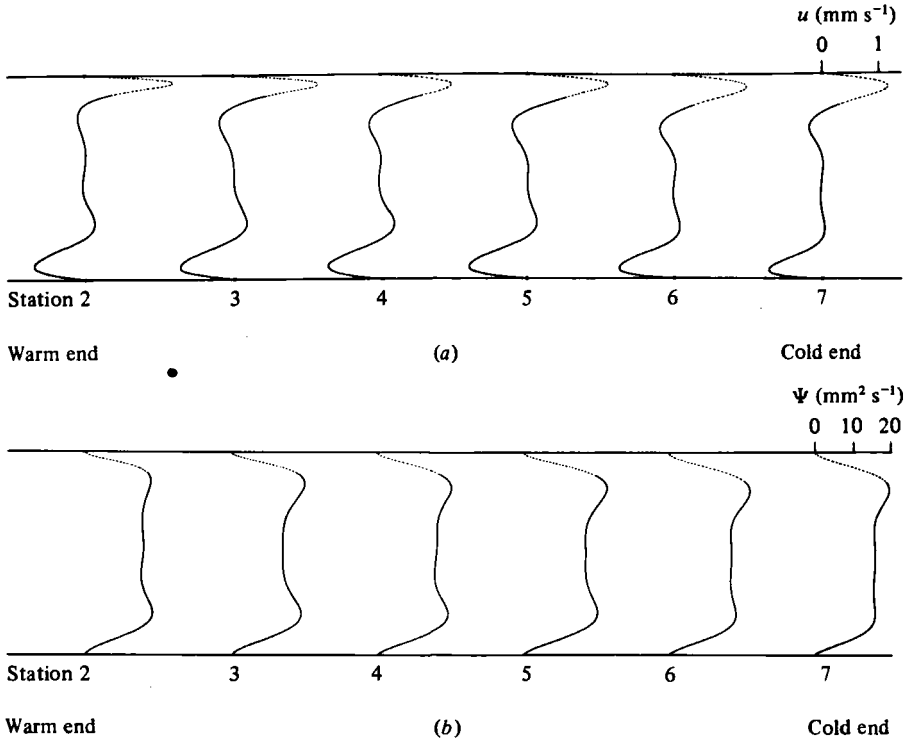

FIGURE 5. (*a*) Horizontal velocity profiles, $Ra = 1{\cdot}59 \times 10^9$, stations 2–7. (*b*) Stream-function calculation based on (*a*).

being nearly constant. Comparing figures 2 and 3 we also find that the vertical temperature gradient increases as the Rayleigh number increases from $1{\cdot}22 \times 10^9$ to $1{\cdot}59 \times 10^9$. The layers located along the top and bottom walls contain fluid decidedly warmer and, respectively, colder than if the central linearly stratified region were to fill the cavity depth entirely. Figure 4(*a*) is the same plot of temperature as given by Imberger (1974), but for a $Ra = 1{\cdot}22 \times 10^9$ ($A^{-4} = 6{\cdot}6 \times 10^4$). The temperature is now constant at mid depth and at $y = 0{\cdot}15$ showing the transition to flow dominated by strong convection.

Figure 4(*b*) shows the dynamics of the vertical temperature distribution as the Rayleigh number increases from 5×10^4 to $1{\cdot}59 \times 10^9$. It is evident that the linearly stratified inner region thickens as Ra increases, at the expense of the two extreme intrusion layers which become thinner.

Velocity measurements outlined in the next section demonstrate that the temperature extremes in the profiles of figures 2, 3 and 4(*b*) are associated with horizontal jet flow in the shallow cavity. The warm jet proceeds along the top of figures 2 and 3, from station 1 to station 8. In the process, the mean jet temperature decays nonlinearly with longitudinal position, as the warm jet loses heat by vertical diffusion to the inner layer and to the horizontal boundary.

In conclusion, the present experiments clearly illustrate the transition to a convectively dominated core flow, with distinct thermal intrusion layers.

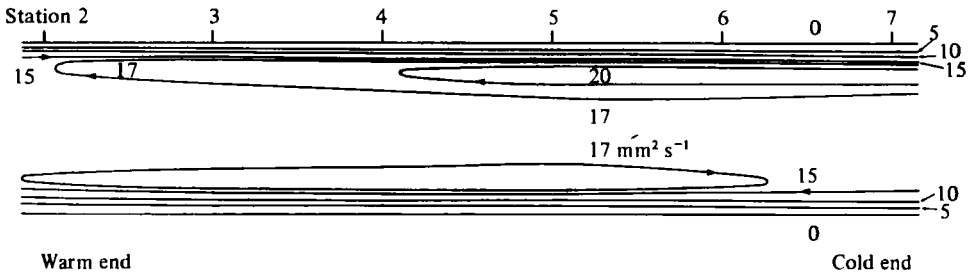

FIGURE 6. Streamline pattern for the core region (stations 2–7), $Ra = 1{\cdot}59 \times 10^9$.

4. Velocity measurements

Flow visualization experiments were conducted at one of the highest Rayleigh numbers achieved in the apparatus, $Ra = 1{\cdot}59 \times 10^9$. The results are condensed in figures 5 and 6. The flow visualization technique consisted of dropping a crystal of potassium permanganate ($KMnO_4$) through an access port and photographically recording the purple streak generated by the falling crystal. Owing to the extreme slenderness of the two-dimensional enclosure, the fluid velocity in the core is for all practical purposes horizontal, so that the deformed purple trajectory assumes the shape of the local horizontal velocity profile. The procedure worked best while using crystals with a diameter of 1 mm and allowing for an average of 40 s before photographing the deformed trajectory.

The horizontal velocity profiles u (mm s^{-1}) corresponding to stations 2–7 have been assembled in figure 5(*a*). Immediately below, in figure 5(*b*), we show the stream function

$$\psi = \int_0^y u\,dy \tag{1}$$

computed from the velocity profiles. Here, y is the vertical position above the horizontal adiabatic wall taken as $y = 0$. It should be noted that the velocity and stream-function profiles are interrupted in the vicinity of the top wall where the crystal first comes in contact with the water space. This initial impact creates a disturbance large enough to affect the top portion of the vertical trajectory described by the crystal. The dotted line is a fourth-order polynomial used to reconstruct the upper portion of the velocity recording. As shown in figure 5(*a*), most of the velocity profile remains unaffected by the entry disturbance.

In figure 6 we sketched a set of streamlines based on the stream function of figure 5(*b*). The flow pattern clearly shows the presence of the district intrusion layers through which most of the fluid circulates. The fluid contained between the two horizontal jets is to a very good approximation stagnant. However, some back flow is discernible as may be expected from Imberger *et al.* (1976).

The streamline pattern of figure 6 and the velocity distribution of figure 5(*a*) indicate a lack of symmetry between the two ends of the core flow. This effect is caused by viscosity variations associated with the temperature difference between the top and bottom horizontal jets.

The velocity measurements reported in figures 5 and 6 can be used to verify the

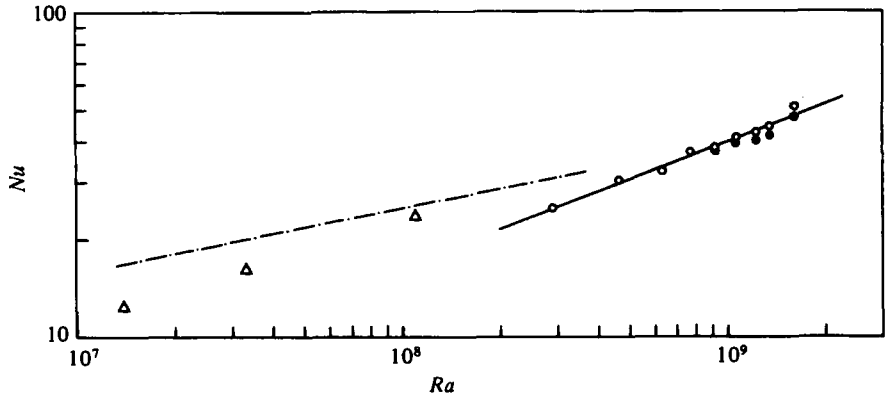

FIGURE 7. Summary of the present heat-transfer results *vis-à-vis* the data published in Imberger (1974) and the theory of Bejan & Tien (1978). △, Imberger (1974), $H/L = 0{\cdot}02$; – · – · –, Bejan & Tien (1978); ○, present results, $H/L = 0{\cdot}0625$; ——, equation (3).

validity of the dimensional analysis presented in § 1. According to Koh (1976), the thickness of the intrusion layer is of the order of $L\,Ra^{-\frac{1}{5}}A^{\frac{2}{5}}$, which in the experiment shown in figure 5 is equal to 0·8 cm. This distance is of the same order as the intrusion-layer thickness measured between the peak-layer velocity and the wall in figure 5(*a*). In addition, the value of the stream function at mid-depth constitutes a measure of the net mass flux in each of the two horizontal jets. According to Gill (1966), the net mass flux should be of the order of κRa; taking $Ra = 1{\cdot}59 \times 10^9$ and the thermal diffusivity of water at 25 °C we find $\kappa Ra \approx 28\,\mathrm{mm^2\,s^{-1}}$, in good agreement with the stream-function result of figure 5(*b*).

In conclusion, the velocity measurements suggest that the picture constructed based on dimensional arguments in § 1 is correct.

5. Heat-transfer results

The net heat exchange in the horizontal direction between the two ends of the cavity is reported in figure 7. The Nusselt number Nu is defined as

$$Nu = \frac{LQ/A}{k(T_h - T_c)}, \tag{2}$$

where Q is the net heat-transfer rate, A the transversal cross-section through the cavity.

Heat-transfer results were obtained in the range $2{\cdot}9 \times 10^8 \leqslant Ra \leqslant 1{\cdot}6 \times 10^9$ and plotted on figure 7 *vis-à-vis* data reported by Imberger (1974) for $Ra \leqslant 1{\cdot}11 \times 10^8$. There is considerable agreement between the two sets of data. The slight discontinuity is attributed to the different aspect ratio used in this experiment, $H/L = 0{\cdot}0625$ versus $H/L = 0{\cdot}02$ in the earlier case. It is evident from figure 7 that the impact of H/L on the Nu–Ra relationship is minor, provided the aspect ratio H/L is much smaller than unity.

The present data are correlated by the following power law obtained by the method of least squares

$$Nu = 0{\cdot}014 Ra^{0{\cdot}38}. \tag{3}$$

It is interesting to note that the exponent on Ra is greater than the value $\frac{1}{4}$ foreseen by Imberger (1974) or the $\frac{1}{5}$ value predicted by Bejan & Tien (1978).

One explanation for the departure of the Ra exponent from the lower theoretical values is the leakage of heat through the upper horizontal wall of the enclosure, as suggested by the temperature profiles shown in figures 2 and 3. We carried out a special experiment to determine the fraction of the warm-end heat input Q lost through the upper wall. The experiment consisted of dissipating a small number of watts (in the range 0–50 W) in the warm-end heaters, with the insulation in place and without water cooling the cold-end jacket. The outside of the cooling jacket was heavily insulated. We attained a number of steady states in which the warm-end heat input was balanced solely by the heat loss from the nearly isothermal enclosure to the ambient. Thus, we were able to simulate upper wall temperatures comparable to the temperatures recorded during the actual experiments; at the same time we recorded the heat loss associated with the water–air heat transfer. On this basis we determined that the heat loss through the upper wall amounts to no more than 9 % of the warm-end heat input.

In figure 7 we show the shift in the Nu–Ra data associated with basing the Nusselt number not on the warm-end heat input (circles) but on the heat input minus the heat loss to the ambient fluid (black dots). It is evident that the measurements at the highest Ra are the ones most affected by this shift. Overall, the shifted data are correlated by

$$Nu = 0{\cdot}028Ra^{0{\cdot}35}, \tag{4}$$

in which the Ra exponent is lower than in equation (3). It is also evident that the highest Ra points now lie on a line of slope closer to $\frac{1}{4}$.

The fact that the Ra exponent is greater than $\frac{1}{4}$ is also the result of heat transfer between the two horizontal branches of the counter-flow, across the thermally stratified core. In the limit $H/L \to 0$, where the vertical heat transfer is dominant, Cormack *et al.* (1974) showed that the Ra exponent is 2. More recently, Bejan (1979) showed that, in the boundary-layer regime with stratified core, the Ra exponent is always of the order of (however, *greater* than) $\frac{1}{4}$: the value $\frac{1}{4}$ is reached asymptotically only as the downward heat transfer across the stratified core becomes negligible.

In closing, the Nu–Ra plot of figure 7 summarizes the limited extent of experimental information on heat transfer in end-to-end heated horizontal enclosures. The graph also shows that more analytical work is needed to explain and, possibly, to predict features of this flow. It is hoped the new flow features reported in this paper will serve as stimulus to further research on this class of phenomena. The current status of *theoretical* research in this area has been reveiwed by Bejan (1980).

6. Concluding remarks

In this paper we summarized the results obtained from an experimental study aimed at uncovering the features of free convection in shallow enclosures in a high-Rayleigh-number range not studied before. The experiment focused on the flow and temperature pattern in the core region.

The temperature and velocity measurements reported here demonstrate that in the range $2 \times 10^8 < Ra < 2 \times 10^9$ the core flow structure is non-parallel. Instead, the core is dominated by the presence of horizontal intrusions lining the two insulated walls

Experiment	A	Ra	Criterion $Ra^{\frac{1}{4}}A$	Remark
Imberger (1974)	0·01	$1{\cdot}31 \times 10^6$ (min)	0·34	No jet
(water, $Pr \simeq 7$)	0·01	$1{\cdot}22 \times 10^7$ (max)	0·59	No jet
	0·019	$8{\cdot}01 \times 10^6$ (min)	1·01	No jet
	0·019	$1{\cdot}11 \times 10^8$ (max)	1·95	Departure from parallel core structure
Kumar & Ostrach (1977)	0·1	3×10^4	1·32	No jet
(silicone, $Pr \simeq 963$)	0·1	$6{\cdot}5 \times 10^4$	1·6	No jet
	0·1	$1{\cdot}1 \times 10^5$	1·82	Weak jet
Present experiment	0·0625	2×10^8 (min)	7·4	Strong jet
(water, $Pr \simeq 7$)	0·0625	$1{\cdot}7 \times 10^9$ (max)	12·7	Strong jet
Loka (1979)	0·2	$1{\cdot}34 \times 10^7$	12·0	Jet
(glycol, $Pr \simeq 1{\cdot}4 \times 10^3$)	0·2	$1{\cdot}8 \times 10^7$	13·0	Jet
	0·1	$1{\cdot}92 \times 10^8$	3·7	Weak jet
	0·05	$2{\cdot}9 \times 10^5$	1·16	No jet

TABLE 1. Available experimental data on natural convection in horizontal enclosures with different end temperatures.

of the enclosure. The inner region bounded by the two jets is occupied by practically stagnant fluid. The fluid temperature in the inner region varies linearly with depth and is independent of longitudinal position. This core structure is therefore similar to that occurring in vertical enclosures in the moderate boundary-layer regime prior to the formation of secondary and tertiary flows (see, for example, Elder 1965; Gill 1966). Another unique feature of the core pattern is the presence of two secondary cells which result from the interaction of the two horizontal jets with the stagnant inner fluid.

The dimensional analysis presented in § 1 yielded the following criterion for the transition from parallel flow in the core region to a flow structure dominated by intrusion layers (jets) lining the two horizontal walls,

$$Ra^{\frac{1}{4}}A < 1, \quad \text{parallel flow (no jet)}, \tag{5}$$

$$Ra^{\frac{1}{4}}A > 1, \quad \text{intrusion layers (jet)}. \tag{6}$$

We verified the validity of this criterion by examining the available experimental data on free convection in shallow enclosures. The existing experiments are summarized in terms of aspect ratio ($A = H/L$) and Rayleigh number (Ra) in table 1, which shows conclusively that criterion $Ra^{\frac{1}{4}}A \lesssim 1$ predicts correctly the core flow structure, in the entire parametric domain covered by experimental observations ($0{\cdot}01 < A < 0{\cdot}2$, $10^4 < Ra < 10^{10}$).

It is worth noting that transition criterion (5, 6) is supported by experimental observation involving a wide Prandtl-number range, $7 \leqslant Pr \leqslant 1400$. It must, however, be remembered that at high Rayleigh numbers not all the flow travels through the vertical boundary layers: some of the flow returns through a modified core flow, giving the impression of a rather large 'viscous' end-region. This effect is clearly seen in the data of Imberger (1974), Kumar & Ostrach (1977) and Loka (1979). In any case, the transition criterion (5, 6) is based on Gill's scaling for vertical end-layers: the

central assumption in this scaling is that the buoyancy forces are balanced by viscous forces, and that inertia is negligible. This postulate requires $Pr \gg 1$, which is a condition met by all the data assembled in table 1.

We conclude that the $Ra^{\frac{1}{4}}A$ criterion predicts correctly the transition from a fully developed counter-flow to two thin layers sandwiching a less active inner region. The streamline pattern in the inner region requires further study. It is quite possible that the complexion of the inner flow, however weak, may depend on the Prandtl number.

The apparatus used in the present experiment was designed and constructed in the Hydraulics Laboratory, Department of Civil Engineering, University of California, Berkeley. The experiments described in this paper were carried out soon afterward in the Department of Mechanical Engineering, University of Colorado, Boulder (see Al-Homoud & Bejan 1979). The financial support received from the National Science Foundation under Grant ENG–7820957 is gratefully acknowledged. The authors also thank Mr Walter Mathews, and Dr D. Perry of Berkeley, and Mr R. Cowgill, Mr K. Rupp, Mr R. Yewell and Professor M. C. Branch of Boulder for their contribution at various stages in this work. Rory Thompson read the final manuscript and made many useful comments.

REFERENCES

AL-HOMOUD, A. A. & BEJAN, A. 1979 Experimental study of high Rayleigh number convection in horizontal cavity with different end temperatures. *Dept Mechanical Engng, Univ. Colorado, Boulder, Rep.* CUMER–79–1.

BATCHELOR, G. K. 1954 Heat transfer by free convection across a closed cavity between vertical boundaries at different temperatures. *Quart. J. Appl. Math.* **12**, 209.

BEJAN, A. 1979 Note on Gill's solution for free convection in a vertical enclosure. *J. Fluid Mech.* **90**, 561.

BEJAN, A. 1980 A synthesis of analytical results for natural convection heat transfer across rectangular enclosures. *Int. J. Heat Mass Transfer* **23**, 723.

BEJAN, A. & TIEN, C. L. 1978 Laminar natural convection heat transfer in a horizontal cavity with different end temperatures. *J. Heat Transfer* **100**, 641.

BOYACK, B. E. & KEARNEY, D. W. 1972 Heat transfer by laminar natural convection in low aspect ratio cavities. *A.S.M.E. Paper* no. 72–HT–2.

BRAUN, W. H., OSTRACH, S. & HEIGHWAY, J. E. 1961 Free-convection similarity flows about two dimensional and axisymmetric bodies with closed lower ends. *Int. J. Heat Mass Transfer* **2**, 121.

CORMACK, D. E., LEAL, L. G. & IMBERGER, J. 1974 Natural convection in a shallow cavity with differentially heated end walls. Part 1. Asymptotic theory. *J. Fluid Mech.* **65**, 209.

CORMACK, D. E., LEAL, L. G. & SEINFELD, J. H. 1974 Natural convection in a shallow cavity with differentially heated end walls. Part 2. Numerical solutions. *J. Fluid Mech.* **65**, 231.

ECKERT, E. R. G. & CARLSON, W. O. 1961 Natural convection in an air layer enclosed between two vertical plates with different temperatures. *Int. J. Heat Mass Transfer* **2**, 106.

ELDER, J. W. 1965 Laminar free convection in a vertical slot. *J. Fluid Mech.* **23**, 77.

GILL, A. E. 1966 The boundary layer regime for convection in a rectangular cavity. *J. Fluid Mech.* **26**, 515.

IMBERGER, J. 1974 Natural convection in a shallow cavity with differentially heated end walls. Part 3. Experimental results. *J. Fluid Mech.* **65**, 246.

IMBERGER, J., THOMPSON, R. & FANDRY, C. 1976 Selective withdrawal from a finite rectangular tank. *J. Fluid Mech.* **78**, 489.

KOH, R. C. Y. 1976 Buoyancy gravitational spreading. *Proc. 15th Coastal Engng Conf. Honolulu.*

KUMAR, A. & OSTRACH, S. 1977 An experimental investigation of natural convection flows in rectangular enclosures of aspect ratios less than unity. *Case Western Reserve Univ., Dept Mechanical Aerospace Engng Rep.* FTAS/TR–77–132.

LOKA, R. R. 1979 Natural convection flows in low aspect ratio rectangular enclosures. M.S. thesis, Dept Mechanical & Aerospace Engng, Case Western Reserve University.

OSTRACH, S. 1972 Natural convection in enclosures. *Adv. Heat Transfer* **8**, 161.

OSTRACH, S., LOKA, R. R. & KUMAR, A. 1980 Natural convection in low aspect ratio rectangular enclosures. Paper presented at the *19th Nat. Heat Transfer Conf., Orlando, Florida.*

SERNAS, V. & LEE, E. I. 1978 Heat transfer in air enclosures of aspect ratio less than one. *A.S.M.E. Paper* no. 78–WA/HT–7.

TSENG, W. F. 1979 Numerical experiments on free convection in a tilted rectangular enclosure of aspect ratio 0·5. M.S. thesis, Dept Mechanical & Industrial Engng, Clarkson College, Potsdam, N.Y. (Rep. no. MIE–050.)